*Sensors and Materials*, Vol. 34, No. 6 (2022) 2325–2340
MYU Tokyo



S & M 2975

# Theoretical Analysis and Experimental Verification of Polytetrafluoroethylene Surface Flashover from Electrostatic Electromagnetic Pulse Field

Yan Zhang,[1] Xin Zhao,[1] Hsiung-Cheng Lin,[2*] Xianghu Ge,[1] and Lu Zhang[1]

[1]College of Electrical Engineering, Hebei University of Science and Technology, Hebei 050018, China
[2]Department of Electronic Engineering, National Chin-Yi University of Technology, Taichung 41170, Taiwan

(Received November 3, 2021; accepted February 21, 2022)

***Keywords:*** PTFE, electromagnetic induction, surface flashover, electrostatic discharge, electrostatic electromagnetic pulse

The insulating material flashover induced by an electrostatic electromagnetic pulse radiation field in a complex electromagnetic environment is a big concern in spacecraft surface materials. Polytetrafluoroethylene (PTFE) is the most often used insulation material in spacecraft. For this reason, the secondary electron emission avalanche (SEEA) model is proposed for the theoretical analyses of and experiments on the PTFE surface flashover induced by an electrostatic electromagnetic pulse radiation field. We use the current probe sensor to measure the induced flashover current waveform on the grounding wire and combine the probability of the electrostatic electromagnetic-pulse-induced flashover under different electrode voltages and electrostatic discharge (ESD) simulator output voltages. First, the SEEA theory is established considering the flashover voltage without an external electrostatic electromagnetic pulse field. The flashover voltage is then applied to the needle-plate electrode, and the distorted electric field is formed at three nodes of electrode–PTFE–air. Second, the flashover voltage with an external electrostatic electromagnetic pulse field is taken into account. The external field producing horizontal and vertical electric field components between the electrodes is fully investigated. Third, experimental results on the electrostatic electromagnetic-pulse-induced PTFE surface flashover using a needle-plate electrode structure are analyzed and discussed in detail. All findings are supported by the proposed SEEA model in an electrostatic protection using PTFE material.

## 1. Introduction

A spacecraft always faces a complex electromagnetic space environment during orbit. Charge and discharge effects may therefore arise from time to time on the surface materials and internal electronic components inside the spacecraft, causing spacecraft malfunction or even failure.[1–3] Some research studies revealed that strong electromagnetic fields in space may not only interfere with spacecraft equipment and operation systems, but also cause flashover from

*Corresponding author: e-mail: hclin@ncut.edu.tw
https://doi.org/10.18494/SAM3724

ISSN 0914-4935 

spacecraft surface materials, thus resulting in serious damage to the operating electronic equipment. The safety of spacecraft operation can be significantly threatened.[4–7] Polytetrafluoroethylene (PTFE) has been widely applied in aerospace materials owing to its excellent corrosion resistance, high temperature resistance, and insulation properties. It is mainly used for the insulation protection of spacecraft solar arrays and various types of electronic equipment.[8–11]

In recent years, relevant research has been mainly focused on the surface flashover characteristics of PTFE materials and the induced conditions of complex space environments.[12–16] Xie and coworkers worked on the static electromagnetic pulse radiation field induced by a needle-ball electrode test under strong electromagnetic and space radiation environments.[17,18] Du *et al.* studied the surface charging and flashover voltage behavior at different temperatures.[19] It was found that the change in surface molecular structure inhibits the accumulation of surface charges, thereby suppressing the distortion of the electric field. It could effectively increase the flashover voltage at different temperatures. Xing *et al.* revealed the effects of material parameters on surface charge characteristics and surface flashover voltages under DC.[20] It was found that the dissipation rate of surface charge increased under low relative permittivity and volume resistivity. Chen *et al.* established an experimental platform to analyze the characteristics of polypropylene film flashover voltage under high-pressure $SF_6$.[21] They showed that the relationship of flashover voltage and gas pressure can be divided into two regions. In low-pressure regions, the flashover voltage increases linearly with the gas pressure, and in high-pressure regions, the increase in flashover voltage gradually slowed down to approach a saturation value.

In response to the above-mentioned problems, we derive and analyze the factors that may affect the occurrence of flash over using the secondary electron emission avalanche (SEEA) model. The designated test system and test samples were used to analyze the induced PTFE materials in the electrostatic electromagnetic pulse environment. The mechanism of the surface flashover has been extensively explored. The charging characteristics of the PTFE surface in the atmospheric environment and the basic law of inducing flashover can be obtained.

## 2. Theory Establishment

### 2.1 Flashover voltage without external electrostatic electromagnetic pulse field

In the SEEA model,[22] when the voltage is applied to the needle-plate electrode, the distorted electric field can be formed at three nodes of electrode–PTFE–air. Initial electrons are emitted by the field at the distorted electric field and are then accelerated by the field so that the surface of the material is hit to emit secondary electrons. The positive charge remains on the surface of the material, thereby generating an electric field $E_{n0}$ perpendicular to the surface of the material. It can be expressed as

$$E_{n0} = \sigma / 2\varepsilon_0, \tag{1}$$

where $\sigma$ is the surface charge density and $\varepsilon_0$ is the free dielectric constant ($8.85 \times 10^{-14}$ F/cm). The angle $\theta$ between the synthetic electric field and the surface of the material can be expressed as

$$\tan\theta = E_{n0} / E_{t0} = \left(2A_0 / \left(A_1 - A_0\right)\right)^{\frac{1}{2}}, \tag{2}$$

where $E_{t0}$ is the horizontal electric field formed by the electrode voltage when flashover occurs; $E_{n0}$ is the vertical electric field on the material surface; $A_1$ is the electron collision energy; $A_0$ is the emitted electron energy (4.7 eV).

The flashover current density $J_0$ on the surface of the material can be expressed as

$$J_0 = \sigma v_e E_{n0} / A_1, \tag{3}$$

where $v_e$ is the average velocity of electrons. In unit area, the critical value ($M_{cr}$) of desorption gas molecules of flashover discharge can be expressed as

$$M_{cr} = \left(\gamma J_0 / q v_0\right) d, \tag{4}$$

where $v_0$ represents the average rate of desorption of gas molecules on the surface of the insulating material; $q$ is the amount of electronic charge; $d$ is the electrode spacing; $\gamma$ is the probability of desorption.

According to the desorption gas theory on the surface of the material[19] and the above formulas, the DC surface flashover breakdown electric field $E_{t0}$ and the flashover threshold voltage $U_s$ can be calculated as

$$E_{t0} = \left(\frac{M_{cr} A_1 v_0 q}{2\varepsilon_0 d \gamma v_e \tan\theta}\right)^{\frac{1}{2}} \tag{5}$$

$$U_s = E_{t0} d = \left(\frac{M_{cr} A_1 v_0 q d}{2\varepsilon_0 \gamma v_e \tan\theta}\right)^{\frac{1}{2}} \tag{6}$$

From Eq. (6), $U_s$ can be obtained without an external electrostatic electromagnetic pulse field. When the applied voltage $U_1$ between electrodes is greater than $U_s$, flashover, also called spontaneous flashover, will occur. When the applied voltage $U_1$ between electrodes is less than $U_s$, no flashover will occur.

### 2.2 Flashover voltage with external electrostatic electromagnetic pulse field

When an electrostatic electromagnetic pulse field is applied, the external field will produce a horizontal electric field component $E_{t1}$ and a vertical electric field component $E_{n1}$ between the

electrodes, as shown in Fig. 1. The angle between $E_{t1}$ and $E_1$ is $\omega$.

From the electromagnetic field theory, the operating range of electrons is confined near the insulator surface owing to the effect of the positive surface charge. Therefore, the electron density $\sigma_-$ cannot be greater than the surface positive charge density $\sigma_+$. On the other hand, $\sigma_-$ cannot be significantly less than $\sigma_+$ when the electron reaches a certain density and drift velocity. As a result, it is reasonable to estimate that the magnitude of $\sigma_-$ is constantly approaching $\sigma_+$. The densities of surface electrons ($\sigma_-$) and positive ions ($\sigma_+$) in PTFE are defined as

$$\sigma_- = \sigma_+ = 2\varepsilon_0 E_{t1} \tan\omega. \tag{7}$$

The horizontal component $v_{0t}$ and vertical component $v_{0n}$ at the initial electron movement velocity are respectively defined as

$$\begin{cases} v_{0t} = \sqrt{2A_0/m_e}\cos\beta, \\ v_{0n} = \sqrt{2A_0/m_e}\sin\beta, \end{cases} \tag{8}$$

where the electron mass is $m_e$. The angle between the initial electron emission direction and the surface of the PTFE material is $\beta$.

Given that the amount of electron charge is $q$, the electron horizontal acceleration $a_t$ and vertical acceleration $a_n$ are defined as

$$\begin{cases} a_t = qE_{t1}/m_e, \\ a_n = qE_{n1}/m_e. \end{cases} \tag{9}$$

When the electron travels to the point of the farthest normal distance from the surface of the insulator, i.e., the farthest vertical distance from the surface of the PTFE, the normal velocity decays to 0. The electron travel time taken is $\Delta t$ and the tangential distance is $\Delta x$, which are respectively expressed as

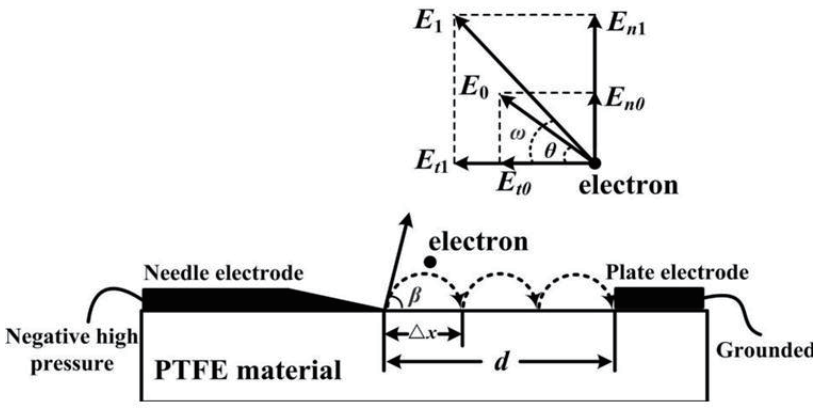


Fig. 1. Field distribution diagram between needle-plate electrodes.

$$\Delta t = \frac{v_{0n}}{a_n} = \frac{\sqrt{2m_e A_0}\sin\beta}{qE_{n1}}, \tag{10}$$

$$\Delta x = v_{0t}\left(2\cdot\Delta t\right) + \frac{1}{2}a_t\left(2\cdot\Delta t\right)^2 = \frac{4A_0}{qE_{n1}^2}\left(E_{n1}\sin\theta\cos\theta + E_{t1}\sin^2\theta\right). \tag{11}$$

When the electron returns to the insulator surface, its normal velocity $v_n$ is equal to the initial normal velocity but with an opposite direction. Therefore, the tangential velocity $v_t$ can be expressed as

$$v_t = v_{0t} + a_t\left(2\cdot\Delta t\right) = \sqrt{\frac{2A_0}{m_e}}\left(\cos\theta + \frac{2E_{t1}\sin\theta}{E_n}\right). \tag{12}$$

During the whole process, electrons move towards the anode to form a flashover current. The tangential flashover current density $J_{t1}$ is determined by the charge density $\sigma_{-}$ and the speed of tangential drift $v_t$, shown as

$$\begin{aligned} J_{t1} &= \sigma_{-}v_t = 2\varepsilon_0 E_{t1}\tan\omega\sqrt{\frac{2A_0}{m_e}}\left(\cos\theta + \frac{2\left|E_{t1}\right|\sin\theta}{\left|E_{n1}\right|}\right) \\ &= 2\varepsilon_0 E_{t1}\tan\omega\sqrt{\frac{2A_0}{m_e}}\left(\cos\theta + 2\mathrm{ctg}\omega\sin\theta\right). \end{aligned} \tag{13}$$

According to the electron tangential movement distance $\Delta x$ derived above, the number of times that electrons hit the surface of the insulation material per unit length is $1/\Delta x$. Accordingly, the normal flashover current density $J_{n1}$ on the insulator surface can be obtained as

$$J_{n1} = J_{t1}\frac{1}{\Delta x}. \tag{14}$$

The desorption rate $\gamma$ of adsorbed gas on the surface of the insulator is directly determined by the density of the electron that hits the surface of the insulator. It is expressed as $\gamma = \sigma_{-}Q/q$, where σ- is adsorbed gas density of the insulator surface, $Q$ is the electron collision cross section, and its average value is $Q = 10^{-16}$ cm$^2$.

Usually, the desorption probability in different materials differs, which can be observed by predicating the outgassing rate in different flashover processes on the surface of the electronically excited insulator. The electron-induced desorption probability in the adsorbed gas is denoted as $\gamma$. The desorption speed $J_1$ of adsorbed gas molecules is defined as

$$J_1 = \frac{\gamma J_{n1}}{q} = \frac{\gamma J_{t1}}{q\Delta x}. \tag{15}$$

The density ($N$) of desorbed gas molecules is expressed as

$$N = \frac{J_1}{v_{gas}} = \frac{\gamma J_{t1}}{q v_{gas}\Delta x}, \tag{16}$$

where $v_{gas}$ is the velocity of the desorbed gas that leaves the insulator surface.

The density ($M$) of desorbed gas molecules on the insulator surface with the needle-plate electrode space ($d$) is

$$M = Nd = \frac{\gamma J_{t1} d}{q v_{gas}\Delta x}. \tag{17}$$

By substituting Eq. (13) into Eq. (17) for further transformation, we can obtain $E_{t1}$ as

$$E_{t1} = \frac{\sqrt{2A_0 m_e}\, v_{gas}\left(\tan\omega\sin\theta\cos\theta + \sin^2\theta\right)}{M\varepsilon_0\gamma d\cdot\tan^3\omega\left(\cos\theta + 2ctg\omega\sin\theta\right)}. \tag{18}$$

The voltage component $U_g$ induced by the applied field between the electrodes can be obtained[23] as

$$U_g = E_{t1}d = \frac{\sqrt{2A_0 m_e}\, v_{gas}\left(\tan\omega\sin\theta\cos\theta + \sin^2\theta\right)}{M\varepsilon_0\gamma\cdot\tan^3\omega\left(\cos\theta + 2ctg\omega\sin\theta\right)}. \tag{19}$$

The voltage condition to generate flashover is expressed as

$$U_{s1} = U_g + U_1 \geq U_s, \tag{20}$$

where $U_1$ is the electrode voltage and $U_s$ is the flashover voltage threshold.

Equation (20) indicates that the flashover is triggered by not only the high-voltage source voltage connected to the needle-plate electrode, but also the voltage component $U_g$ induced by the external field between the electrodes. At this time, flashover can occur only if $U_g \geq U_s - U_1$ is satisfied.

According to Ref. 23, when conducting the contact electrostatic discharge (ESD) experiment with reference to IEC 61000-4-2, the electrostatic electromagnetic pulse field has random field strength in the near field. This may lead to the inconsistent field strength and direction of the electrostatic electromagnetic pulse emitted under the same ESD simulator output voltage. It has

low repeatability each time but higher repeatability in the far field. However, the field strength is very small in this case so that it is not conducive to the judgment of induced flashover. To judge whether the electrostatic electromagnetic pulse can induce flashover more accurately, the near-field area with a larger field strength for experiments should be chosen.

## 3. Experimental System and Device Design

### 3.1 Establishment of experimental system

According to the International Electrotechnical Commission standard IEC 61000-4-2, a flashover experimental platform using a needle-plate electrode structure was established under an atmospheric environment, as shown in Fig. 2. It was mainly composed of an ESD simulator, an induced discharge experimental platform, and a temperature and humidity control monitoring system.

The discharge gun in the ESD simulator was used for the noncontact discharge of the coupling plate to generate an electrostatic electromagnetic pulse radiation field, which acts as a background electromagnetic field on the test unit to induce a flashover effect. By adjusting the voltage between the needle and plate electrodes ($U_1$) on the surface of the PTFE material and the output voltage of the ESD simulator ($U_2$), the flashover between high-voltage electrodes on the surface of the insulation material can be investigated. The regularity of PTFE flashover characteristics can thus be obtained.

### 3.2 Experimental device

The experiments performed on the PTFE surface electrode structure (shown in Fig. 3) have three major parts. The first part is the electrostatic electromagnetic pulse field generator, which

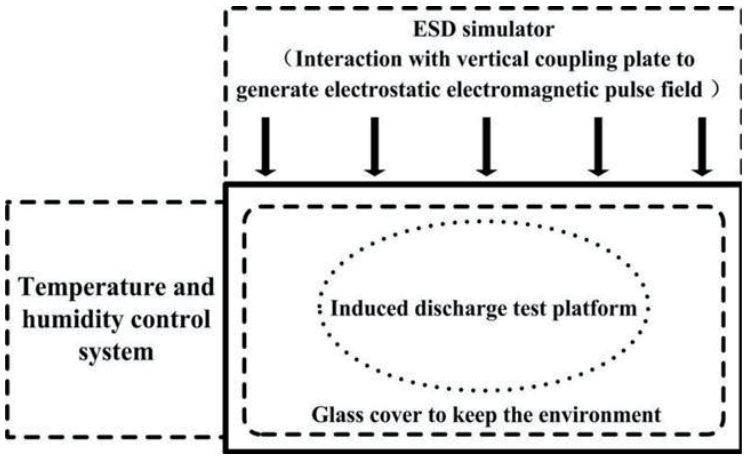


Fig. 2. Schematic of experimental system.

is composed of an electrostatic discharge simulator using an ESS-200AX ESD simulator [i.e., numbers 1 and 2 in Fig. 4(a)] and a vertical metal coupling plate [i.e., number 3 in Fig.4(a)]. The second part is a high-voltage source using GLOW 28720 DC high-voltage power supply to be applied between the electrodes [i.e., number 4 in Fig. 4(a)]. The third part is the flashover detection device, including the Tektronix TDS7404B oscilloscope of Tektronix Company, Tektronix CT-1 current probe (volt–ampere output characteristic: 5 mV/1 mA), and 30 dB attenuator [i.e., number 8 in Fig. 4(a)], to be equipped to protect experimental equipment. Therefore, the current signal can be detected when the insulation material flashover is induced.

The test unit was placed in the environmental control device, as shown in Fig. 4(b), where the ambient temperature was set as 20 °C with 40% RH. During the experiment, the flashover current acquisition device was overcurrent-protected by connecting 30 dB attenuators in series.

In this experiment, the electrostatic electromagnetic pulse radiation field was used to simulate the spatial radiation field, and PTFE was used as the insulation material. The needle-plate electrode simulated the possible discharge electrode structure on the surface of the insulation material. The electrostatic electromagnetic pulse radiation field was generated to induce flashover, and the discharge current signal value was then measured.

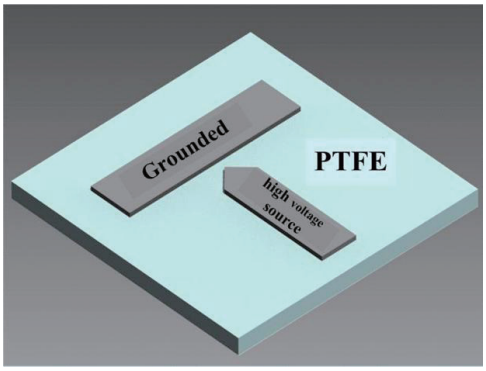


Fig. 3. (Color online) Electrode structure on PTFE surface.

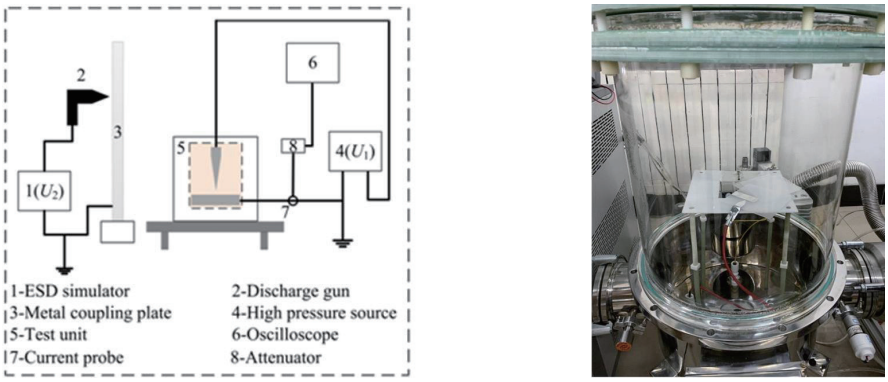


(a) (b)

Fig. 4. (Color online) Experimental system and unit under test. (a) Induced flashover test system. (b) Induced flashover test unit.

## 4. Experimental Results and Analysis

### 4.1 Experimental process

The experiment was carried out in the atmospheric environment. The discharge gun of the ESD simulator discharged the vertical metal coupling plate in a noncontact manner to generate the electrostatic electromagnetic pulse radiation field, which acted on the test unit as the experimental background field. The electrostatic electromagnetic pulse radiation field with different field intensities was simulated by changing the voltage $U_2$ output by the ESD simulator. To reduce the experimental error and avoid the effect of the charging time, the electrostatic electromagnetic pulse field was applied 60 times with 2 s intervals. For fair evaluation, the first 20 times and the last 20 times were removed, and only the middle 20 experiments were retained. The data were then sorted out to determine the number of successful flashovers, and the probability of inducing flashovers, that is, the ratio of the number of successfully induced flashovers to the number of electrostatic electromagnetic pulse fields, was calculated. In addition, PTFE samples were replaced each time to avoid the variation of surface insulation characteristics caused by the flashovers. The experimental steps are demonstrated as follows.

Step 1: By adjusting the DC high voltage source connected by the needle-plate electrode on the surface of the PTFE material, the voltage $U_1$ between the needle and the plate electrode is changed to induce the flashover on the surface of the PTFE material. At this time, the voltage added by the needle-plate electrode is the initial threshold of the flashover. To verify whether the electrostatic electromagnetic pulse field induces flashover, the applied voltage $U_1$ between the needle and plate electrodes should not exceed this threshold.

Step 2: Decrease $U_1$ to 0 V and continuously use the electrostatic electromagnetic pulse field to irradiate the test unit. Increase $U_1$ until flashover occurs and then measure the flashover voltage. On this basis, keep the ESD simulator output voltage $U_2$ unchanged. Adjust $U_1$ and observe the induced flashover to formulate the induced law.

Step 3: Decrease the electrode voltage $U_1$ below the natural flashover voltage threshold. Then, keep $U_1$ unchanged, but change $U_2$. Observe the number of induced flashovers and formulate the induced law under different values of the ESD simulator output voltage $U_2$.

From this experiment, the probability of the electrostatic electromagnetic pulse inducing flashover on PTFE can be analyzed and summarized under different values of the electrode voltage $U_1$ and ESD simulator output voltage $U_2$.

### 4.2 Determination of induced flashover

The flashover current signals generated on the surface of the PTFE material using the needle-plate electrode are shown in Fig. 5. Under different values of the ESD simulator output voltage $U_2$ and electrode voltage $U_1$, the spontaneous flashover current waveform is as shown in Fig. 5(a) when $U_1 = -2.9$ kV and $U_2 = 0$ kV. No electrostatic electromagnetic pulse field was applied and

the electrode voltage reached the flashover voltage threshold. The current waveform caused by the electromagnetic induction of the electrostatic electromagnetic pulse field is shown in Fig. 5(b) when $U_1 = 0$ kV and $U_2 = -30$ kV without electrode voltage. The induced flashover currents at $U_1 = -2.8$ kV and $U_2 = -30$ kV, $U_1 = -2.6$ kV and $U_2 = -30$ kV, $U_1 = -2.4$ kV and $U_2 = -25$ kV, and $U_1 = -2.0$ kV and $U_2 = -15$ kV are shown in Figs. 5(c)–5(f), respectively. The marks A–E in Figs. 5(b)–5(f) indicate the dividing points between two different waveforms. In Fig. 5(b), the first section waveform before point A is the attenuation oscillation current induced by the electrostatic electromagnetic pulse radiation field in the discharge circuit. The second attenuation

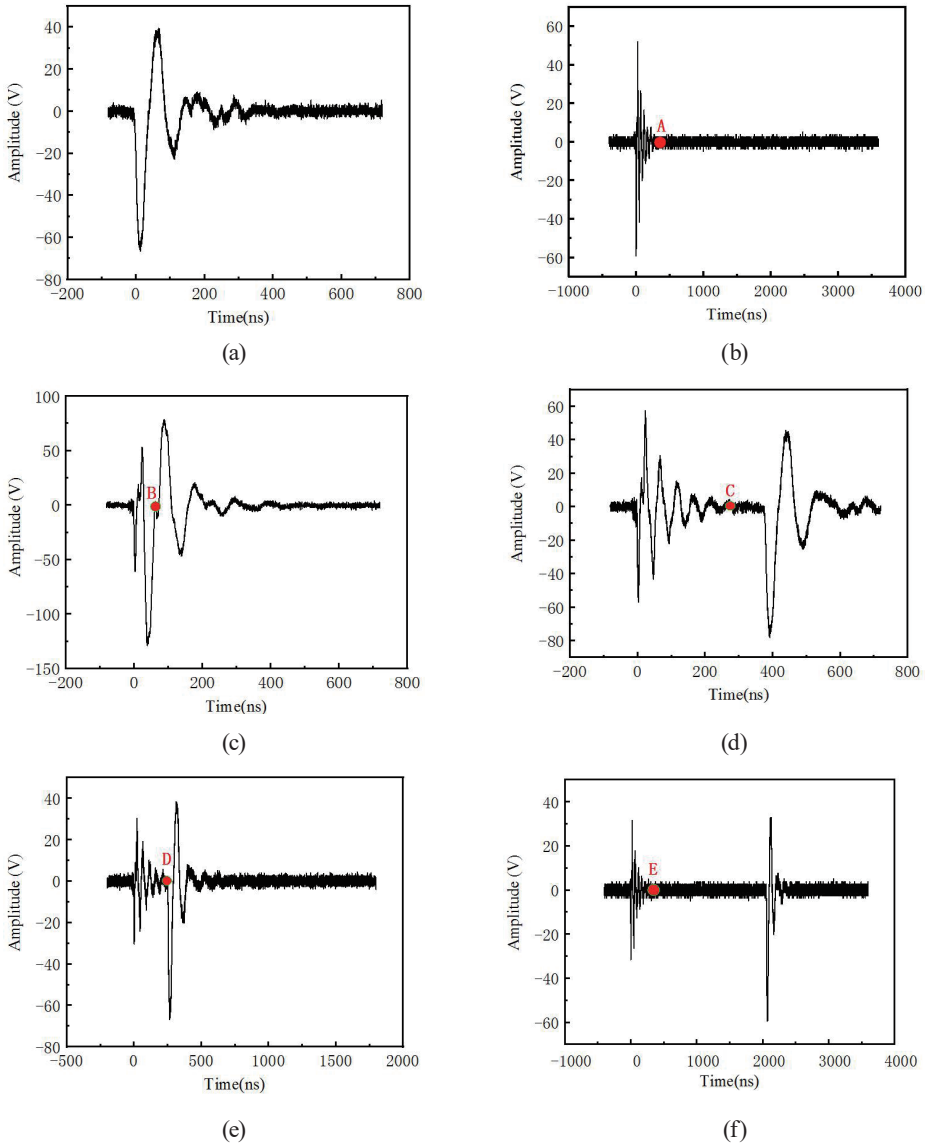


Fig. 5. (Color online) Induced flashover currents under different conditions. (a) Spontaneous flashover current at $U_1 = -2.9$ kV and $U_2 = 0$ kV. (a) Induced current at $U_1 = 0$ kV and $U_2 = -30$ kV. (c) Induced flashover current at $U_1 = -2.8$ kV and $U_2 = -30$ kV. (d) Induced flashover current at $U_1 = -2.6$ kV and $U_2 = -30$ kV. (e) Induced flashover current at $U_1 = -2.4$ kV and $U_2 = -25$ kV. (f) Induced flashover current at $U_1 = -2.0$ kV and $U_2 = -15$ kV.

oscillation waveform after point A is the flashover current induced by the electrostatic electromagnetic pulse radiation field. When the electrode voltage is 0 kV and the ESD simulator voltage is −30 kV, only the electromagnetic induction current waveform of the electrostatic electromagnetic pulse is generated, and no flashover current waveform is generated after point A. Similarly, the oscillation waveform before points B–E represents the current waveform generated by the electromagnetic induction of the electrostatic pulse in the discharge unit and the grounding circuit. The oscillation waveform after points B–E represents the flashover current waveform. Moreover, points B–E are depicted as the location where the induced current attenuates to zero. As above, it can be seen that the higher the output voltage of the ESD simulator, the larger the amplitude of the induced discharge current waveform. In Fig. 5, note that the induced current directly measured from the scope current probe is exhibited using voltage amplitude (V), where the relation between the voltage and current amplitudes is 5 mV/1 mA.

### 4.3 Rules of induced flashover

The relationship between the induced flashover probability and the electrode voltage $U_1$ at $U_2$ = −30 kV is shown in Fig. 6. From this relationship, $U_1$ was taken as −1.6, −1.7, −1.8, −2.0, −2.2, and −2.4 kV. It reveals that the induced flashover probability increased abruptlywhen it ranged from −1.7 to −1.8 kV. The flashover probability became 100% since $U_1$ = −2.0 kV. Also, the probability of inducing flashover is close to zero when the electrode voltage is −1.6 kV. If the electrode voltage is 0 kV, the electric field intensity will be lower. Therefore, the induced voltage generated by the radiation field at both ends of the electrode will be less than the flashover voltage of the insulating material. Under this situation, it can be deduced that the induced flashover probability is zero, and the flashover current waveform will not be generated at this time. This corresponds to the current waveform of electromagnetic induction shown in Fig. 5(b), where there is no flashover waveform.

The relationship between the induced flashover probability and the ESD simulator voltage $U_2$ is shown in Fig. 7, where the electrode voltage $U_1$ was set as −2.0, −2.4, −2.6, and −2.8 kV. It can be seen that, under the same electrode voltage, as the ESD simulator absolute output voltage $U_2$

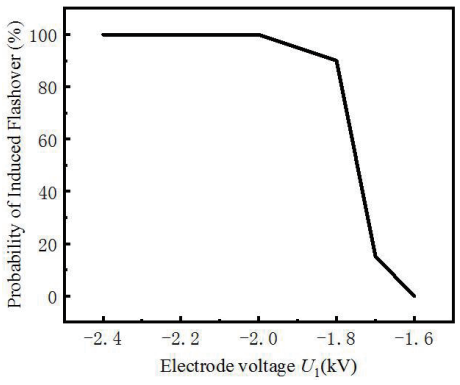


Fig. 6. Relationship between induced flashover probability and electrode voltage $U_1$.

increases, the probability of inducing flashover increases. When the output voltage $U_2$ is between −10 and −25 kV, higher electrode voltage levels can achieve higher induced flashover probabilities. When the output voltage of the ESD simulator is between −25 and −30 kV, all flashovers are completely induced regardless of the electrode voltage. It is clear that the probability of inducing flashover can be affected by both the output voltage $U_2$ and the electrode voltage $U_1$.

At $U_1$ = −2.8 kV, the induced flashovers at $U_2$ = −10, −5, and −2 kV are shown in Fig. 8. Note that a $U_2$ value higher than −25 kV can produce flashover with a sufficient electrostatic electromagnetic pulse radiation field since the first flashover. It can be seen that at $U_2$ = −10, −5, and −2 kV, the electrostatic electromagnetic pulse was irradiated at the thirteenth, eighteenth, and twenty-sixth times, respectively, when the first flashover occurred. As above, this implies that the higher the output voltage $U_2$ the ESD simulator provides, the smaller the number of irradiations is required to induce flashover for the first time. This explains the charge accumulation effect on the needle-plate electrode and the surface of the PTFE material when the test unit is irradiated with an electrostatic electromagnetic pulse radiation field. The higher the output voltage $U_2$ the ESD simulator provides, the more charges of each electrostatic electromagnetic pulse irradiation accumulate. Therefore, it can reach the flashover threshold earlier, and then the flashover occurs.

At $U_2$ = −20 kV, the induced flashovers are shown in Fig. 9 at $U_1$ = −2.8, −2.4, −2.0, and −1.6 kV. It can be seen that at $U_1$ = −2.8, −2.4, −2.0, and −1.6 kV, the electrostatic electromagnetic pulse was irradiated at the second, third, ninth, and thirty-seventh times, respectively, when the first flashover occurred. The results show that the higher the $U_1$ value, the smaller the number of irradiations required for the first flashover to occur. This explains that the higher the $U_1$ value across the electrode, the greater the intensity of the distorted electric field formed at the electrode–PTFE–air triple node. This leads to increases in the number and speed of initial electrons, the acceleration of the electrons placed in the field, and the generation of secondary electrons when the electrons are accelerated to hit the material surface. Accordingly, less irradiation times are taken to accumulate more electrons.

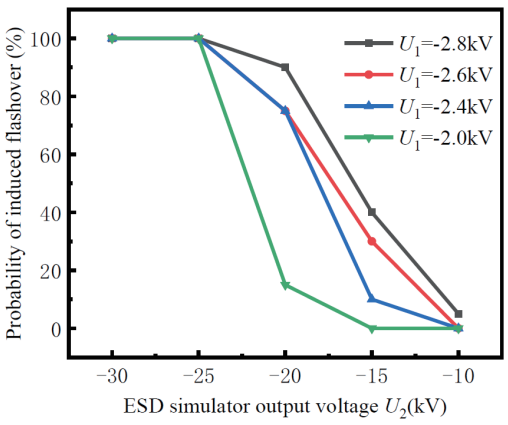


Fig. 7. (Color online) Relationship between induced flashover probability and ESD simulator voltage $U_2$.

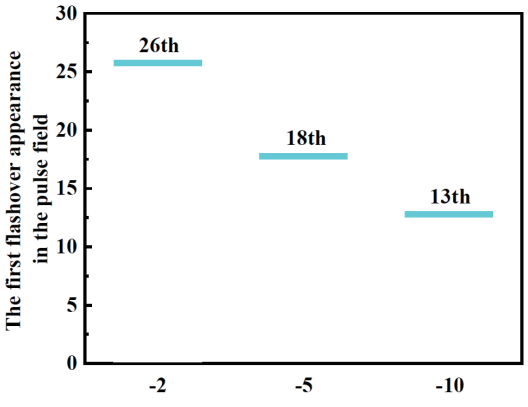


Fig. 8. (Color online) Induced flashovers under different ESD voltages.

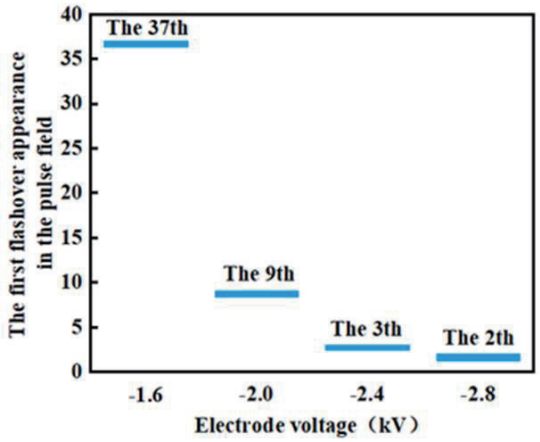


Fig. 9. (Color online) Induced situations under different electrode voltages.

### 4.4 Analysis and summary of induced flashover mechanism

According to the experimental results mentioned above, some crucial points can be concluded as follows.

1) In the absence of an external electrostatic electromagnetic pulse field, the applied electrode voltage $U_1$ can form a distorted electric field at the electrode–PTFE–air triple junction. The flashover voltage threshold $U_s = -2.9$ kV was obtained by the experimental method. When the electrode voltage is far greater than the flashover voltage, i.e., $U_1 >> U_s$, the distorted electric field at the three nodes of electrode–PTFE–air is sufficiently strong, which leads to a large number of initial electrons emitted. The electrons are then accelerated to generate flashover. When the electrode voltage is less than the flashover voltage, i.e., $U_1 < U_s$, the distorted electric field intensity at the electrode–PTFE–air triple node is low, that is, the electric field intensity $E_{t0}$ does not reach the threshold of the breakdown field strength. Therefore, the acceleration and accumulation kinetic energies of electrons are insufficient to generate flashover.
2) When an electrostatic electromagnetic pulse field is applied, the distorted electric field at the three nodes can emit initial electrons. According to the flashover voltage condition, i.e., $U_{s1} = U_g + U_1 \geq U_s$, when the electrode voltage is much higher than the flashover voltage, i.e., $U_1 >> U_s$, flashover will occur directly. When the electrode voltage is less than the flashover voltage, i.e., $U_1 < U_s$, flashover will not occur with the electrode voltage $U_1$ only. However, the horizontal component $E_{t1}$ of the applied field will produce the induced voltage $U_g$ between the electrodes. If the sum of the voltage $U_g$ and the electrode voltage is far greater than the flashover voltage threshold $U_s$, i.e., $U_g + U_1 > U_s$, flashover will be induced.

According to the experiment results, it is clear that increasing the field strength of the electrostatic electromagnetic pulse field can fundamentally improve the probability of the induced flashover. For example, the electrode voltage $U_1$ is adjusted to −2.0 kV when the output voltage $U_2$ of the ESD simulator is −30 kV, and the probability of flashover induced by applying an electrostatic electromagnetic pulse is 100%, where $U_g + U_1 >> U_s$. When the output voltage

$U_2$ of the ESD simulator is −20 kV, the probability of induced flashover decreases to about 18%, where $U_g + U_1 \geq U_s$. When the ESD simulator output voltage is $U_2 = -10$ kV, the probability of induced flashover is 0%, where $U_g + U_1 < U_s$.

It can be concluded that the flashover voltage condition to induce flashover is $U_{s1} = U_g + U_1 \geq U_s$. However, the field strength of each emission may not be completely consistent,[24] which may lead to the randomness of the induced voltage $U_g$. With a sufficiently large applied electrostatic electromagnetic pulse field, the probability is determined by the following situations:

a. When the electrostatic electromagnetic pulse field strength is far greater than the induced critical field strength, the induced potential $U_g >> U_s - U_1$ can be guaranteed, and the probability of induced flashover is 100%.
b. When the field strength of the electrostatic electromagnetic pulse is near the induced critical field strength, the induced potential $U_g > U_s - U_1$ cannot be guaranteed owing to the randomness of the electrostatic electromagnetic pulse field.
c. When the electrostatic electromagnetic pulse field strength is less than the induced critical field strength, the induced potential $U_g < U_s - U_1$, and the induced probability is 0%.

### 4.5 Induced flashover in vacuum environment

Desorption is to excite gas molecules from a low energy state to a high energy state through electron energy transfer and electron excitation so that the gas molecules can overcome the adsorption force of dielectric surface molecules to be released. When electrons collide with the adsorbed gas on the surface of the medium, electron energy is transferred to gas molecules. Assuming an elastic collision between electrons and adsorbed gas molecules, according to the energy conservation theorem, the maximum kinetic energy $E_{max}$ of gas molecules is

$$E_{max} = 4E_e \frac{Nm}{(m+M)^2} \approx 4E_e \frac{N}{M}, \tag{21}$$

where $M$ is the mass of the gas molecule; $m$ is the mass of the electron; $E_e$ is the electron energy. Since $M >> m$, $M + m \approx M$. When electrons collide inelastically with gas molecules, the energy $E$ of gas molecules is

$$E = E_e \frac{m}{M}. \tag{22}$$

According to Eqs. (21) and (22),[25] the energy transfer is very small, and the electron energy transfer also has little effect on gas desorption. Therefore, the desorption that occurred mainly by electron excitation results in a phenomenon that the gas molecules break away from the solid surface binding.

In the atmospheric environment, the background ambient gas plays a role in the material flashover process along the surface. The average free path of electrons is less than the electrode spacing, and the desorption gas content on the material surface is very small compared with the

background gas content. When the air pressure enters the high vacuum stage, the background gas content decreases considerably, and the desorption gas on the material surface becomes the main reaction gas in the formation of flashover. It can be seen from Eq. (6) that both the critical value of desorption gas molecules and the average velocity of molecular desorption will affect the flashover voltage. In a vacuum environment, the higher the average velocity of gas molecule desorption, the higher the flashover voltage will be. Therefore, electrostatic electromagnetic pulses with higher intensities are needed to induce flashover, causing a higher induced flashover voltage of insulating materials in a vacuum environment than in an atmospheric environment.

## 5. Conclusions

In this study, the experimentally induced flashover platform using electrostatic electromagnetic pulse field irradiation has been established on the basis of the SEEA model. The surface needle-plate electrode structure was also designed to carry out the experiment on the surface of the PTFE material. The major contributions are concluded as follows.

1) How the flashover phenomenon is induced by electrostatic electromagnetic pulse field irradiation on the surface of PTFE has been demonstrated.
2) Through theoretical analysis, the crucial factors that may affect the flashover voltage threshold are obtained. Therefore, the electrode voltage threshold inducing flashover can be determined under a certain electrostatic electromagnetic pulse field strength.
3) Under a constant electrode voltage, the field-induced voltage between the electrodes increases as the electrostatic electromagnetic pulse field strength increases. Accordingly, the increased induced voltage is then superimposed on the electrode voltage to increase the probability of flashover.
4) With a constant strength in the electrostatic electromagnetic pulse field, the voltage between the electrodes is closer to the flashover voltage threshold as the electrode voltage increases. At this time, the probability of inducing flashover increases gradually.
5) In the vacuum environment, because the content of the excited gas is far less than that in the atmosphere, the flashover generated by the electronic excitation requires a higher electrostatic electromagnetic pulse intensity. As a result, the induced flashover voltage of insulating materials in the vacuum environment is higher than that in the atmosphere.

The experimental results have supported the theoretical analysis of the PTFE surface flashover induced from an electrostatic electromagnetic pulse field. Indeed, it provides a valuable guide for the applications of insulating materials in spacecraft under a low-orbit environment.

## References

1 J. F. Ma, W. J. Dong, C. X. Zhang, J. J. Liu, C. M. Zhou, and J. Y. Lin: Proc.2017 1st Int. Conf. Electronics Instrumentation & Information Systems (IEEE, 2017) 1–5. https://doi.org/10.1109/EIIS.2017.8298751
2 N. Pothier: Proc.2017 Asia-Pacific Int. Symp. Electromagnetic Compatibility (IEEE, 2017) 266–268. https://doi.org/10.1109/APEMC.2017.7975479
3 P. Xiao, H. He, J. J. He, C. Cheng, and M. Xiao: Proc.2018 IEEE Int. Conf. High Voltage Engineering and Application (IEEE, 2018) 1–4. https://doi.org/10.1109/ICHVE.2018.8641922

4 T. Shahsavarian, C. Li, M. A. Baferani, and Y. Cao: Proc. 2020 IEEE Conf. Electrical Insulation and Dielectric Phenomena (IEEE, 2020) 271–274.https://doi.org/10.1109/CEIDP49254.2020.9437456
5 S. Fukushige, Y. Akahoshi, K. Watanabe, T. Nagasaki, K. Sugawara, T. Koura, and M. Cho: IEEE Trans. Plasma Sci. **36** (2008) 2434. https://doi.org/10.1109/TPS.2008.2004960
6 T. Zhuang, X. Gao, M. Ren, S. Wang, and J. Huang: Proc. 2019 IEEE Electrical Insulation Conf. (IEEE, 2019) 469–472. https://doi.org/10.1109/EIC43217.2019.9046591
7 L. Liu, X. A. Li, Q. G. Zhang, C. J. Liang, H. Y. Ren, J. P. Zhao, and Z. B. Li: Proc. 2018 IEEE Int. Conf. Electrical Insulation and Dielectric Phenomena (IEEE, 2018) 255–258. https://doi.org/10.1109/CEIDP.2018.8544732
8 M. Y. Wang, B. X. Du, J. Li, Z. L. Li, M. Xiao, and Y. Q. Xing: Proc. 2020 IEEE Int. Conf. Applied Superconductivity and Electromagnetic Devices (IEEE, 2020) 1–2. https://doi.org/10.1109/ASEMD49065.2020.9276130
9 W. Zha and Q. Qiu: Proc. 2019 IEEE 3rd Int. Electrical and Energy Conf. (IEEE, 2019) 26–30. https://doi.org/10.1109/CIEEC47146.2019.CIEEC-201938
10 G. Zhang, G. Su, B. Song, and H. Mu: IEEE Trans. Dielectr. Electr. Insul. **25** (2018) 2321. https://doi.org/10.1109/TDEI.2018.007133
11 J. Chintalapalli, J. Ndikumana, S. K. Baang, and J. Park: Sens. Mater. **32** (2020) 3373. https://doi.org/10.18494/SAM.2020.2776
12 S. Li, S. Pan, G. Li, D. Min, W. Wang, and S. Li: IEEE Trans. Dielectr. Electr. Insul. **24** (2017) 1288. https://doi.org/10.1109/TDEI.2017.006103
13 S. Q. Hou, Y. R. Qin, J. X. Gao, F. Y. Lyu, and X. F. Li: Sens. Mater. **33** (2021) 1127. https://doi.org/10.18494/SAM.2021.2974
14 H. C. Miller: IEEE Trans. Dielectr. Electr. Insul. **22** (2015) 3641. https://doi.org/10.1109/TDEI.2015.004702
15 Y. Gao, Z. Li, H. Wang, and X. Yuan: IEEE Trans. Dielectr. Electr. Insul. **27** (2020) 998. https://doi.org/10.1109/TDEI.2019.008634
16 C. Ren, J. Wang, P. Yan, L. Xiao, T. Wang, and D. Zhang: IEEE Trans. Dielectr. Eletr. Insul. **20** (2013) 1189. https://doi.org/10.1109/TDEI.2013.6571433
17 X. N. Xie, X. J. Hu, Q. Y. Yuan, S. H. Liu, and J. P. Zhang: Proc. 2019 IEEE 6th Int. Symp. Electromagnetic Compatibility (IEEE, 2019) 1–4. https://doi.org/10.1109/ISEMC48616.2019.8986140
18 X. N. Xie, X. F. Hu, and Q. Y. Yuan: Proc. 2019 Int. Conf. Electronic Engineering and Informatics (IEEE, 2019) 206–212. https://doi.org/10.1109/EEI48997.2019.00052
19 B. X. Du, R. R. Xu, J. Li, H. L. Liu, M. Xiao, Z. L. Li, and Z. H. Hou: Thin Solid Films **680** (2019) 12. https://doi.org/10.1016/j.tsf.2019.04.025
20 Z. L. Xing, C. P. Li, C. Zhang, Z. Zhang, W. K. Li, J. S. Ru, Y. Xiao, Y. Zhou, and X. Chen: Proc.2017 1st Int. Conf. Electrical Materials and Power Equipment (IEEE, 2017) 184–187. https://doi.org/10.1109/ICEMPE.2017.7982062
21 Z. Q. Chen, W. Jia, F. Guo, J. N. Li, W. Wu, and S. C. Ji: Proc. IEEE Trans. Plasma Sci. (IEEE, 2019) 4553–4559. https://doi.org/10.1109/TPS.2019.2917829
22 A. S. Pillaian and R. Hackam: J. Appl. Phys. **53** (1982) 2983. https://doi.org/10.1063/1.331037
23 W. Gao and Z. H. Wang: J. Insu. Mater. **41** (2008) 56. https://doi.org/10.16790/j.cnki.1009-9239.im.2008.04.016
24 J. Liu, Y. G, Chen, Z. L. Tan, and M. J. Li: High Volt. Eng. **38** (2012) 435. https://kns.cnki.net/kcms/detail/detail.aspx?FileName=GDYJ201202027&DbName=CJFQ2012
25 X. Ma, W. Gao, G. S. Sun, and P. Yan: Electr. Eng. **5** (2006) 38. https://kns.cnki.net/kcms/detail/detail.aspx?FileName=DQJS200605011&DbName=CJFQ2006